20th Australasian Fluid Mechanics Conference
Perth, Australia
5-8 December 2016

Turbulence modifications in a turbulent boundary layer over spanwise-alternating roughness lanes

H.L. Bai[1, 2], Kevin[1], N. Hutchins[1] and J.P. Monty[1]

[1]Department of Mechanical Engineering
University of Melbourne, Victoria 3010, Australia

[2]Department of Civil and Environmental Engineering
Hong Kong University of Science and Technology, Clear Water Bay, Kowloon, Hong Kong

Abstract

Turbulence modifications over a rough wall with spanwise-varying roughness are investigated at $Re_\tau \approx 2{,}000$, using particle image velocimetry (PIV) and hotwire anemometry. The rough wall is comprised of spanwise-alternating longitudinal lanes of two different roughness heights (with a ratio of 8 between the high and low roughness heights). The width of the high-roughness lanes is half of that of low-roughness ones. PIV measurements are performed in a wall-parallel plane located in the logarithmic region, while hotwire measurements are made in a cross-stream plane. In a time-averaged sense, Large-scale counter-rotating roll-modes, are observed in the cross-stream plane over the rough wall, with downwash and upwash common flows displayed over the high- and low-roughness lanes, respectively. Meanwhile, elevated and reduced streamwise velocities occur over the high- and low-roughness lanes, respectively. Significant modifications of Reynolds stresses and vortex activities are also observed, which will be presented in the conference talk.

Introduction

Much work so far has been focused on turbulent flows over a rough wall with a sudden step change along the streamwise direction [1]. One of the dominant features in these flows is that internal boundary layers, associated with distinct integral length scales and Reynolds stresses, were generated immediately downstream of the roughness transition location. In contrast, turbulent flows over a rough wall with transverse roughness transitions (i.e., the roughness change is parallel, instead of perpendicular, to the free stream direction) have received less attention in the literature. The transverse roughness transition not only occurs in nature such as in a riverbed [2], but also was encountered in mechanical engineering such as over a turbine blade damaged by depositions of foreign materials [3]. The latter surface is characterized by a broad range of topographical scales arranged in a highly irregular manner. Time-invariant upwelling and downwelling common flows were observed over the smooth (or relatively low-roughness) and rough (or relatively high-roughness) strips or patches, respectively [2,3]. Correspondingly, these common flows created low- and high-momentum pathways (termed as LMPs and HMPs, respectively), extending to the outer region of the TBL. Further, these LMPs and HMPs exhibit a spanwise-alternating arrangement over the rough wall, with the former flanked by a pair of counter-rotating swirling motions. Spanwise heterogeneities of turbulent statistics (such as Reynolds stresses and turbulent kinetic energy) were produced, which are internally linked to the transverse roughness transitions [3]. Recently, Willingham et al. [4] deployed alternating longitudinal strips of different roughness along the spanwise direction and performed, using large eddy simulation (LES), a detailed parametric study of a turbulent channel flow over this transverse-varying roughness. Two parameters were examined: (i) the ratio (λ) between the high and low roughness heights from λ = 2 to 900; and (ii) the width (L_{hr}) of the high-roughness strip from L_{hr} = 0.2 to 1δ, where δ is a specified boundary layer thickness. Large δ-scaled secondary flows were observed, i.e., large-scale swirling motions centered approximately over the transition, with associated upwash flow over the low-roughness strips and downwash flow over the high-roughness strips, together with large spanwise variations of the streamwise mean velocity. These observations were ascribed to the turbulent mixing induced by the abrupt variation of wall shear stress on the borders of the roughness transitions. Nevertheless, in their LES the equilibrium logarithmic law was applied to the near wall region to compute the imposed aerodynamic drag on the flow by the rough wall. Further experimental studies are indispensable to document the large-scale secondary flows observed over the rough wall with transverse roughness transitions.

This paper reports results from our experimental investigation of the TBL formed over a surface comprised of transverse-varying roughness. Similar to [4], the rough wall is configured by streamwise-aligned and spanwise-alternating sandpaper strips of two different roughness heights. The ratio of high and low roughness heights is λ = 8 and the former has a width 0.5 times the latter. The techniques of PIV and hotwire anemometery are employed to measure the modified flows over the rough wall.

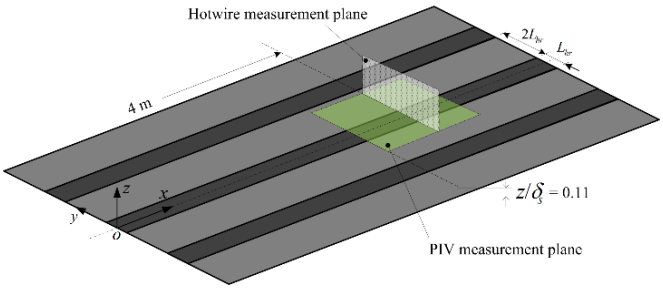

Figure 1. Arrangements of PIV and hotwire measurements over the rough wall. The dark and light shades indicate high- and low-roughness lanes, respectively. The high-roughness lane has a width L_{hr} = 50 mm or 0.91δ_s, where δ_s denotes the boundary layer thickness over the counterpart smooth wall at the same downstream locations (x = 4m) from the leading edge.

Experiments

Rough Wall and Wind Tunnel

Figure 1 illustrates the schematic of the rough wall formed by spanwise-alternating longitudinal lanes of two different roughness. The high-roughness lane (width L_{hr} = 50 mm) is a 40-grit sandpaper with average grit diameter $\bar{d}$ = 425 μm, and the low-roughness lane ($2L_{hr}$) is a 240-grit sandpaper with $\bar{d}$ = 53 μm, yielding a ratio between the high and low roughness $\lambda \approx 8$. There are a total of 3 high-roughness lanes and 4 low-roughness lanes across the width of the facility. The sandpaper lanes have the same

substrates, ensuring that topographical transition along the spanwise direction is only due to the difference in roughness. The rough wall covers the entire width and 6 m length of the wind tunnel from the inlet to the working section.

Experiments are conducted in an open-loop blower-type wind tunnel which has a 6.7 m-long test section of 0.94 m × 0.375 m (width × height) at The University of Melbourne. The tunnel ceiling has a slightly divergent angle, which is adjustable to ensure a zero-pressure gradient along the streamwise direction in the test section. Parts of the ceiling are embedded with glass to permit optical access. A smooth or rough wall can be conveniently placed on the tunnel floor. The flow entering the working section is tripped by a strip of 40-grit sandpaper glued immediately at the exit of the contraction section. The TBL is developed over the tunnel floor. The incoming free-stream velocity (U_∞) is monitored at x = 5.4 m downstream from the exit of the contraction section using a Pitot-static tube and a pressure gauge (Baratron, 698A11TRA). The Pitot-static tube has an internal diameter of 4 mm. The pressure gauge has a measurement range of 10 Torr, with a reading accuracy of 0.1%. Nominal U_∞ is 15.0 m/s, with a free-stream turbulent intensity < 0.7%. PIV and hotwire measurements (see details later) are mainly carried out at 4 m downstream of the working section inlet, where the TBL over the smooth wall has a thickness δ_s = 55 mm (based on the $0.99U_\infty$ location), a friction velocity U_τ = 0.55 m/s (based on fitting hotwire data to direct numerical simulation data in the near-wall region), and a Reynolds number $Re_\tau = \delta_s U_\tau/\nu$ = 1,985, where ν is the kinematic viscosity of air.

The origin of the coordinate system is located at the centreline of the rough wall (Fig 1), with the streamwise, spanwise and wall-normal directions designated by x, y and z, respectively. The streamwise mean and fluctuating velocities are denoted by $\bar{U}$ and u, respectively, while the spanwise and wall-normal mean velocities are denoted by $\bar{V}$ and $\bar{W}$, respectively.

PIV and Hotwire Measurements

PIV measurements are conducted in a wall-parallel plane located at z/δ_s = 0.11 in the logarithmic region (Fig 1). Two overlapping light sheets approximately 1 mm thick, produced by a pair of Nd:YAG pulsed lasers, are employed to illuminate the flow. The laser has a wavelength of 532 nm, a maximum output energy of 200 mJ and a repeating rate of 1 Hz. Each laser pulse has a duration of 10 ns. The flow is seeded with Polyamide (DEHS) droplets of about 1 μm in diameter generated by a fog generator. Particle images are captured using two frame-straddled charge-couple-device (CCD) cameras (PCO4000, 4008 × 2672 pixels each) deployed side-by-side on top of the tunnel and normal to the light sheets. The field of view has an area of 190 mm × 150 mm (width × length), i.e., $3.4\delta_s \times 2.7\delta_s$, covering both the high- and low-roughness lanes along the spanwise direction. Flow illumination and image capturing are synchronized via timing units which have 1 ns resolution. A full 2D calibration is performed using a target marked with laser etched dots (diameter = 1 mm) spaced by 5 mm in both x and y directions. Spatial cross-correlation is performed to calculate the velocity vectors using an in-house PIV package. To reduce contamination by the reflection from the sandpaper grit, the background of the raw images are removed through subtracting their average. An interrogation window of 16 pixel × 16 pixel (i.e., 22 × 22 wall units) is adopted, with 50% overlapping in both directions. The spurious vectors are removed by means of local standard deviation. Only velocity fields with spurious vectors < 2.5% of the total number of vectors are considered valid and thus used in the following analysis. Around 3,800 realizations are obtained, ensuring converged 1st and 2nd-order statistics within ±1% uncertainty.

A miniature single-wire probe (55P15, Dantec) and an X-wire probe (55P61, Dantec), operated on an in-house Melbourne University constant temperature anemometer (MUCTA), are used to measure streamwise velocity U (and hence $\bar{U}$ and u), and the cross-stream $\bar{V}$ and $\bar{W}$, respectively. The sensing element is a Platinum wire of 5 μm diameter, and approximately 1 mm etched length for the single- and X-wires. An overheat ratio of 1.8 is used. The hotwire probes are mounted on an in-house 2 axis traverse moveable in both y- and z-directions (i.e., in the cross-stream plane, Fig 1). The z-direction movement is encoded by a linear encoder (RoHS, P201-9Q) with a resolution of 0.1 μm. For the single-wire hotwire measurement, there are a total of 21 × 44 measurement stations covering an area of Δy = 200 mm (i.e., $3.6\delta_s$) and z = 0.5–100 mm (i.e., $1.8\delta_s$) in the yz-plane; for the X-wire hotwire measurement, the grid is 29 × 31 covering Δy = 180 mm (i.e., $3.2\delta_s$) and z = 6–100 mm (i.e., $1.7\delta_s$). The measurement grids are logarithmically spaced in the z-direction for both measurements. Pre- and post-calibrations are performed in the free stream using the Pitot-static tube. Signals from the hotwires are offset, amplified and sampled at 30 kHz using a 16-bit analogue-to-digit convertor (Data Translation DT9836). The sample duration of the signals is 40 s at each grid point, corresponding to a turn-over time in the TBL of around $11{,}000\delta_s/U_\infty$.

Results

Instantaneous Flows

Representative instantaneous streamwise fluctuating velocities (u^+) in the logarithmic region (at z/δ_s = 0.11) over the rough wall are presented in Fig 2, with the smooth wall case provided for a comparison purpose. The superscript '+' denotes normalization by the inner variables over the smooth wall. It can be seen that, in Fig 2(b) the flow structures over the smooth wall are characterized by streamwise-elongated velocity streaks. These streaks display longitudinally a meandering fashion, with the low-speed streaks flanked by similarly sized high-speed events. Similar observations can be made for the flow structures over the rough wall (Fig 2a). The low- and high-speed streaks exhibit the typical meandering and side-by-side feature; their occurrence seems very random when visually going through all the PIV realizations from the present measurement.

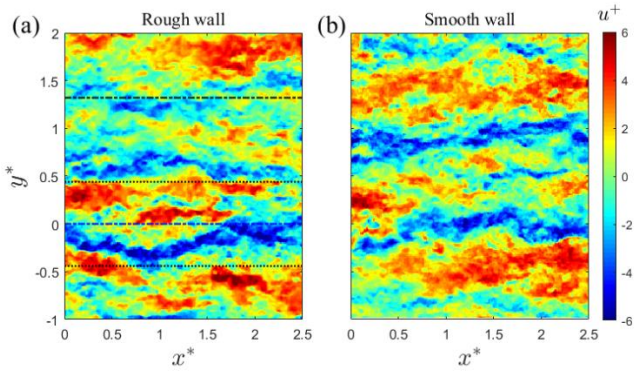

Figure 2. Instantaneous streamwise fluctuating velocities (u) at z/δ_s = 0.11 in the logarithmic region over (a) the rough and (b) smooth walls. The black and blue dot-dashed lines in (a) indicate the centrelines of the low- and high-roughness lanes, respectively; and the black dotted lines indicate the borders of the rough lanes.

Wall-parallel Mean Flows

Figure 3 presents time-averaged velocities ($\bar{U}^*$ and $\bar{V}^*$) of the wall-parallel plane in the logarithmic region (at z/δ_s = 0.11) over the rough wall. The superscript '*' denotes normalization by the outer variables, i.e., U_∞ and δ_s. What can be seen immediately in Fig 3 is the considerable variations of $\bar{U}^*$ and $\bar{V}^*$ along the

spanwise direction. Elevated $\overline{U}^*$ occurs largely over the high-roughness lane, whereas reduced $\overline{U}^*$ takes place over the middle part of low-roughness lanes (Fig 3a). Compared with the smooth wall case (Fig 3b), the $\overline{U}^*$ is increased over the high-roughness lane, with two maxima identified at the locations of borders between the high- and low-roughness lanes. On the contrary, $\overline{U}^*$ is reduced over the middle part of the low-roughness lane. Similar observations were made in [3,4]. In Fig 3(c) & (d), increased and reduced $\overline{V}^*$ is recognized in the proximity of the borders; with $\overline{V}^*$ having opposite signs on different sides of the high-roughness lane. These behaviours of $\overline{V}^*$ indicate that lateral flows are produced, in a time-invariant sense, over the rough wall comprised of spanwse-varying roughness. This may be ascribed to the sudden change of roughness at the borders [4].

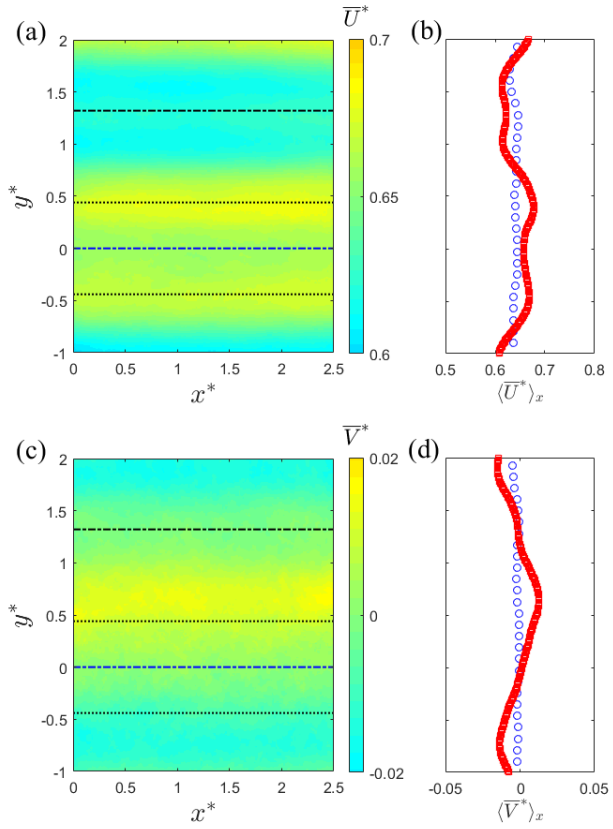

Figure 3. Time-averaged streamwise ($\overline{U}$, a & b) and spanwise ($\overline{V}$, c & d) velocities at z/δ_s = 0.11 in the logarithmic region over the rough wall. The symbol $\langle\ \rangle_x$ indicates ensemble average along the streanwise x direction. The open markers in (b) and (d) are for the smooth wall case. The black and blue dot-dashed lines in (a) and (c) indicate the centrelines of the low- and high-rough lanes, respectively; and the black dotted lines indicate the borders of the rough lanes.

Cross-stream Mean Flows

Time-averaged streamwise ($\overline{U}^*$), spanwise ($\overline{V}^*$) and wall-normal velocities ($\overline{W}^*$) from the hotwire measurements are presented in Fig 4. The high-roughness lane is located at $|y^*| \leq 0.45$, while the low-rough lanes at $|y^*| > 0.45$; the centres of the latter are at $|y^*| = 1.5$. Spanwise variations are evidently notable for all three components of velocity in the cross-stream plane. In Fig 4(a), $\overline{U}^*$ is largely elevated / reduced over the high- / low-roughness lanes, respectively, which is consistent with the observations from the wall-parallel PIV data (Fig 3a). As a result of this, there is a significant change of the boundary layer thickness (δ) along the spanwise direction. Compared to δ_s, δ is increased by about 3% at the centre of high-roughness lane ($y^* = 0$), but by about 25% at the centres of the low-roughness lanes ($|y^*| = 1.5$). The spanwise-averaged δ is on average increased, i.e., about 18% larger than δ_s.

For the in-plane $\overline{V}^*$ component (Fig 4b), one can see its anti-symmetric distribution about the vertical line at $y^* = 0$. In the region of $z^* < 0.3$, $\overline{V}^*$ is negative and positive at the left and right sides of $y^* = 0$, respectively, which is consistent with observations from the wall-parallel PIV measurements in the logarithmic region (Fig 3c). Furthermore, $\overline{V}^*$-distribution exhibits reversed signs in the region $z^* > 0.3$, further indicating lateral flows throughout the boundary layer. In Fig 4(c), the wall-normal $\overline{W}^*$ is negative, largely over the high-rough lane, indicating a predominant downwash, while appearing to be positive over the low-roughness lane.

The behaviours of $\overline{V}^*$ and $\overline{W}^*$ clearly imply that there are circulation motions within the boundary layer over the rough wall. This is confirmed by the distributions of velocity vectors ($\overline{V}^*$, $\overline{W}^*$) given in Fig 5. Evidently, a pair of counter-rotating roll-modes is generated in the cross-stream plane. The motions have a scale comparable to the boundary layer thickness. There is a common-flow down associated with the reduced streamwise velocity $\overline{U}$ in the logarithmic region in between the roll-modes, i.e., over the high-roughness lane. Meanwhile, a common-flow up is produced by the roll-modes, associated with elevated $\overline{U}$ in the log region, over the low-roughness lanes.

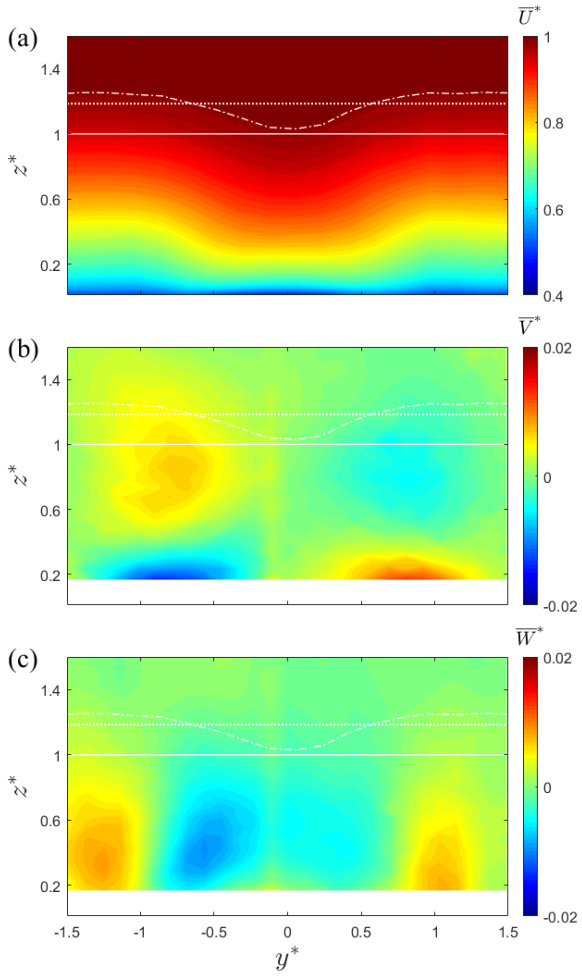

Figure 4. Time-averaged (a) streamwise ($\overline{U}$,), (b) spanwise ($\overline{V}$) and (c) wall-normal ($\overline{W}$) velocities from hotwire measurements in the cross-stream plane at x = 4 m downstream of the working section inlet (c.f. Fig 1). The white dot-dashed curve denotes the boundary layer thickness over the rough wall; and the white solid and dotted lines indicate the spanwise-averaged boundary layer thickness over the smooth and rough walls, respectively.

Conclusions

Wall-parallel PIV and cross-stream hotwire measurements have been conducted to investigate the modified turbulent flows over a rough surface comprised of spanwise-varying roughness strips. The sudden change of roughness is realized by spanwise-alternately deploying longitudinal lanes of two different roughness, with the ratio of 8 between the grit size of the high and low roughness. Considerable variations along the spanwwise direction have been observed for the velocity components and the boundary layer thickness. Large-scale secondary flows, in terms of time-averaged counter-rotating roll-modes, are generated, which is associated with increased and reduced streamwise velocities over the high- and low-roughness lanes, respectively. It is worth noting that the secondary flows are only really readily available in a time-averaged sense, and instantaneously the effect of the spanwise variation in roughness is more difficult to see from the PIV snapshots. A more thorough investigation of the turbulent structure over this rough surface will be given in the full presentation.

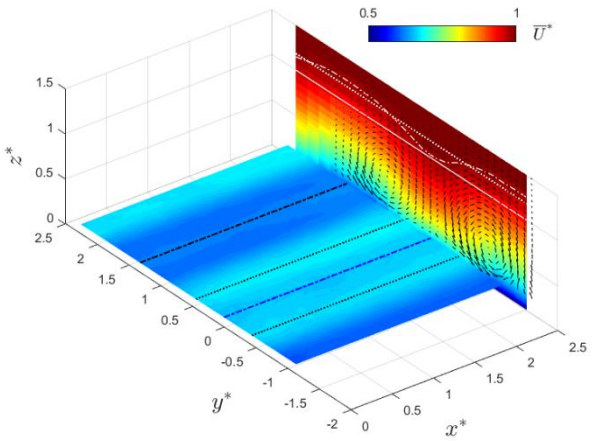

Figure 5. Time-averaged streamwise velocity $\overline{U}$ from PIV measurements in the wall-parallel plane (at z/δ_s = 0.11) and from hotwire measurements in the cross-stream plane (at 4 m downstream of the leading edge). Time-averaged velocity vectors ($\overline{V}$, $\overline{W}$) from the hotwire measurements are included to facilitate data interpretation. In the wall-parallel plane, the black and blue dot-dashed lines indicate the centrelines of the low- and high-rough strips, respectively; and the black dotted lines indicate the borders of the strips. In the cross-stream plane, the dot-dashed curve denotes the boundary layer thickness over the rough wall; and the solid and dotted lines indicate the spanwise-averaged boundary layer thicknesses over the smooth and rough walls, respectively.

Acknowledgments

The authors are grateful for the financial support by the Australian Research Council.

References

[1] Antonia, R.A. & Luxton, R.E., The response of a turbulence boundary layer to a step change in surface roughness. Part I. Smooth to rough, J. Fluid Mech., **48**, 1971, 721-761.

[2] Wang, Z.-Q. & Cheng, N.-S., Time-mean structure of secondary flows in open channel with longitudinal bedforms, *Adv. Water Resour*., **19**, 2006, 1634-1649.

[3] Mejia-Alvares, R. & Christensen, K.T., Wall-parallel stereo particle-image velocimetry measurements in the roughness sublayer of turbulent flow overlying highly irregular roughness, *Phys. Fluids*, **25**, 2013, 115109.

[4] Willingham, D., Anderson, W., Christensen, K.T. & Barros, J.M., Turbulent boundary layer flow over transverse aerodynamic roughness transition: Induced mixing and flow characterization, *Phys. Fluids*, **26**, 2014, 025111.